

Characterization of Majorana-Ising phase transition in a helical liquid system

Sudip Kumar Saha¹, Dayasindhu Dey¹, Monalisa Singh Roy¹, Sujit Sarkar² and Manoranjan Kumar¹

¹ S. N. Bose National Centre for Basic Sciences, Block - JD, Sector - III, Salt Lake, Kolkata - 700106, India

² Poornaprajna Institute of Scientific Research, 4 Sadashivanagar, Bangalore 560080, India

E-mail: sudipksaha@bose.res.in, dayasindhu.dey@gmail.com, singhroy.monalisa@gmail.com, sujit.tifr@gmail.com, manoranjan.kumar@bose.res.in

Abstract. We map an interacting helical liquid system, coupled to an external magnetic field and s-wave superconductor, to an XYZ spin system, and it undergoes Majorana-Ising transition by tuning of parameters. In the Majorana state lowest excitation gap decays exponentially with system size, and the system has degenerate ground state in the thermodynamic limit. On the contrary, the gap opens in the Ising phase even in the thermodynamic limit. We also study other criteria to characterize the transition, such as edge spin correlation with its neighbor $C(r = 1)$, local susceptibility χ_i , superconducting order parameter of edge spin $P(r = 1)$, and longitudinal structure factor $S(k)$. The ground state degeneracy and three other criteria lead to the same critical value of parameters for Majorana-Ising phase transition in the thermodynamic limit. We study, for the first time, the entanglement spectrum of the reduced density matrix of the helical liquid system. The system shows finite Schmidt gap and non-degeneracy of the entanglement spectrum in the Ising limit. The Schmidt gap closes in the Majorana state, and all the eigenvalues are either doubly or multiply degenerate.

Keywords: Majorana fermion, DMRG, helical liquid, Heisenberg model

1. Introduction

The unique properties of the Majorana fermion behaving as its own anti-particle and the existence of particle and anti-particle in the same system are the subjects of intense research interest in various branches of physics, especially in quantum many-body systems since its proposal by E. Majorana [1–3]. The recent studies show that the concept and existence of Majorana, a zero energy mode, like quasi-particles is very common in many branches of physics. Interestingly, it appears as an emergent particle in various condensed matter systems, such as Bogoliubov quasi-particle in a one-dimensional superconductor [4–7], semiconductor quantum wire [8–14], proximity induced topological superconductor [15–24], and the cold atoms trapped in one-dimension [25, 26]. Other than the exotic physics of this topological state, the absence of decoherence in Majorana fermionic system makes it a prospective candidate for application in the non-abelian quantum computation [15, 27–29].

The real world applications of these fermionic systems depend on the stability of the Majorana fermions. A single spin polarized fermion band system with spin orbit coupling and proximity induced superconductor shows Majorana like modes in the presence of weak fermionic interaction. However, it was shown that the interaction weakens the stability of the Majorana fermion [30]. Potter and Lee [21] showed that the $p + ip$ superconductor possesses localized Majorana particles in a rectangular system with width less than the coherence length of the superconductor. The helical liquid system is another candidate where the Majorana like quasi-particles can exist. The helical liquid system generally originates because of the quantum spin Hall effect in a system with or without Landau levels. In this system, a coupling of the left moving down spin with the right moving up spin at the edge of two dimensional quantum hall systems gives rise to a quantized transport process. In this phase, the spin and the momentum degrees of freedom are coupled together without breaking the time reversal symmetry. Various aspects of helical spin liquid is discussed in [31–35].

The field theoretical calculation by Sela et al. [31] shows that the Majorana bound state in a helical liquid possesses a higher degree of stability. In presence of the interaction, the scattering processes between the two constituent fermion bands in the helical liquid

system stabilizes the Majorana bound state by opening a gap [22, 30–32]. However, the strong interaction may induce decoherence in the Majorana modes. They also considered a highly anisotropic spin model with transverse and longitudinal fields, and the system shows Majorana to Ising transition (MI) [31, 32, 35]. One of our coauthors showed using RG calculation that a transition from a phase with Majorana edge modes to the Ising phase exists in the helical liquid system for both presence and absence of interaction [32]. However, a systematic and accurate calculation of the phase boundary of the MI quantum phase transition is still absent in the literature.

In this paper, we study the existence of Majorana fermion modes in the interacting helical liquid system, and also propose different criteria to characterize the MI quantum phase transition. We will also analyze the entanglement spectrum (ES) to characterize the topological aspects of the Majorana edge modes.

Sela et al. [31] introduced a helical fermionic system, which can be written in the field theoretical representation as

$$H = H_0 + \delta H + H_{fw} + H_{um}, \quad (1)$$

where H_0 and δH terms include the kinetic energy, single potential energy, external magnetic field, and proximity induced energy terms. H_{fw} and H_{um} represent the forward scattering and the umklapp scattering terms respectively. The H_0 and δH terms can be written as

$$H_0 = \int dx \left[\psi_{L\downarrow}^\dagger (v_F i \partial_x - \mu) \psi_{L\downarrow} + \psi_{R\uparrow}^\dagger (-v_F i \partial_x - \mu) \psi_{R\uparrow} \right],$$

$$\delta H = \int dx \left[B \psi_{L\downarrow}^\dagger \psi_{R\uparrow} + \Delta \psi_{L\downarrow} \psi_{R\uparrow} + h.c. \right], \quad (2)$$

where Ψ are field operators, v_F and μ are the Fermi-velocity and chemical potential of the helical liquid. The system is coupled to the magnetic field B , and proximity coupled to s -wave superconducting gap Δ which is shown by additional terms in the Hamiltonian. Both the scattering terms are given as

$$H_{fw} = \int dx \left[g_2 \psi_{L\downarrow}^\dagger \psi_{L\downarrow} \psi_{R\uparrow}^\dagger \psi_{R\uparrow} + \frac{g_4}{2} \left\{ \left(\psi_{L\downarrow}^\dagger \psi_{L\downarrow} \right)^2 + \left(\psi_{R\uparrow}^\dagger \psi_{R\uparrow} \right)^2 \right\} \right],$$

$$H_{um} = g_u \int dx \left[\psi_{L\downarrow}^\dagger \partial_x \psi_{L\downarrow} \psi_{R\uparrow}^\dagger \partial_x \psi_{R\uparrow} + h.c. \right]. \quad (3)$$

The conventional analytical expression for the umklapp scattering term H_{um} for the half filling [31, 32, 35, 36] is written in (3). This analytical expression gives a regularized theory using the lattice constant a as an ultraviolet cut-off.

This complete Hamiltonian $H + \delta H + H_{fw} + H_{um}$ can be mapped to a spin-1/2 XYZ model Hamiltonian [31, 32, 35] and can be written as [31]

$$H_i = \sum_i J^\alpha S_i^\alpha S_{i+1}^\alpha - [\mu + B(-1)^i] S_i^z, \quad (4)$$

where $\alpha \equiv x, y, z$ and J^α are different components of spin exchange interaction between neighboring spins. μ and B are longitudinal normal and staggered magnetization applied externally. Here, we assume $J^x = J + \Delta$ and $J^y = J - \Delta$ where Δ is the superconducting gap. Equation (4) can be rewritten in terms of new variables as

$$H = \frac{J}{2} \sum_i (S_i^+ S_{i+1}^- + S_i^- S_{i+1}^+) + J^z \sum_i S_i^z S_{i+1}^z + \frac{\Delta}{2} \sum_i (S_i^+ S_{i+1}^+ + S_i^- S_{i+1}^-) - \sum_i [\mu + B(-1)^i] S_i^z$$

To have a better understanding of the Majorana modes, we map this spin system to the spinless fermion model using Jordan-Wigner transformation [37] of (5), and it can be written in terms of spinless fermion as [38]

$$H = \frac{-J}{2} \sum_i (c_i^\dagger c_{i+1} + h.c.) + J^z \sum_i \left(c_i^\dagger c_i - \frac{1}{2} \right) \left(c_{i+1}^\dagger c_{i+1} - \frac{1}{2} \right) + \frac{\Delta}{2} \sum_i (c_{i+1}^\dagger c_i^\dagger + h.c.) - \sum_i [\mu + B(-1)^i] \left(c_i^\dagger c_i - \frac{1}{2} \right). \quad (6)$$

For the sake of completeness, let us try to understand the results in the limiting cases. This model is well studied in the limit of $B = 0$ and $J^z = 0$, and (6) reduces to 1D Kitaev model [15, 39] which is given by

$$H = -\frac{J}{2} \sum_i (c_i^\dagger c_{i+1} + h.c.) + \frac{\Delta}{2} \sum_i (c_{i+1}^\dagger c_i^\dagger + h.c.) - \mu \sum_i \left(c_i^\dagger c_i - \frac{1}{2} \right). \quad (7)$$

Now let us consider a transformation $c_j = \frac{1}{2}(a_{2j-1} + ia_{2j})$ and $c_j^\dagger = \frac{1}{2}(a_{2j-1} - ia_{2j})$. Here, a_j^\dagger and a_j are the creation and annihilation operators of j^{th} Majorana fermion. We can write (7) as

$$H = \frac{i}{2} \sum_j [-\mu a_{2j-1} a_{2j} + \frac{1}{2} (J + \Delta) a_{2j} a_{2j+1}$$

$$+ \frac{1}{2} (-J + \Delta) a_{2j-1} a_{2j+2}]. \quad (8)$$

There are two conditions: first, when $J = \Delta = 0$ and $\mu < 0$, system shows trivial phase and two Majorana operators at each site are paired together to form a ground state with occupation number 0. Secondly, for $J = \Delta > 0$ and $\mu = 0$, the Majorana operators from two neighboring sites are coupled together leaving two unpaired Majorana operators at the two ends, and these two Majorana modes are not coupled to the rest of the chain [15, 19]. The fermionic edge state formed with these two end operators has occupation 0 or 1 with degenerate ground state, i.e., generating zero energy excitation modes. However, the bulk properties of these systems can be gapped.

In most of the papers [22, 40–43], the Majorana zero modes (MZM) are characterized by exponential decay of the lowest excitation gap with system size, and a large expectation value of the creation operator of the fermion $\langle GS | c^\dagger | GS \rangle$ near the edges of the system. However, in the spin language there is no trivial relation between the Majorana mode and spin raising operators. Therefore, in this paper our main focus is to find the accurate phase boundary of the MI transition, and for this purpose we focus on the lowest excitation gap Γ , derivative of longitudinal spin-spin correlations $C(1)$ between edge spin and its nearest neighbor spin, and spin density ρ_e of edge sites. In principle, the MZM do not couple with the bulk states [15, 19]; therefore, this correlation of the edge spin should decay exponentially. We notice that a local magnetic susceptibility χ_i shows a discontinuity near the phase transition. Fifth quantity is $P(r)$ of edge spin, and it is similar to the spin quadrupolar/spin-nematic order parameter [44–46] or superconducting order parameter of model in (6). The structure factor $S(q)$ gives us information about the phase boundary and the bulk state. Based on the above quantities the MI transition boundary is calculated in this paper. The bulk properties of the Majorana state is rarely discussed in the literature, however we will try to discuss those properties in this paper. In later part of this paper, the ES of both states are also discussed to understand the topological aspects of Majorana modes.

The Hamiltonian mentioned in (5) is solved using the Density matrix renormalization group (DMRG) [47, 48] and the exact diagonalization (ED) method. The DMRG method is a state of the art numerical technique to solve the 1D interacting system, and is based on the systematic truncation of irrelevant degrees of freedom in the Hilbert space [47, 48]. This numerical method is best suited to calculate a few low lying excited states of strongly interacting quantum systems accurately. To solve the interacting Hamiltonian for ladder and chain with periodic boundary condition, the DMRG

method is further improved by modifying conventional DMRG method [49] for zigzag chains [50], quasi one dimension [51] and higher dimensions [52]. The left and right block symmetry of DMRG algorithm for a XYZ-model of a spin-1/2 chain in a staggered magnetic field (in (5)) is broken. Therefore, we use conventional unsymmetrized DMRG algorithm [47, 48] with open boundary condition. In this model, the total S^z is not conserved as S^z does not commute with the Hamiltonian in (5). As a result, the superblock dimension is large. We keep $m \sim 500$ eigenvectors corresponding to the highest eigenvalues of the density matrix to maintain the desired accuracy of the results. The truncation error of density matrix eigenvalues is less than 10^{-12} . The energy convergence is better than 0.001% after five finite DMRG sweeps. We go upto $N = 200$ sites for the extrapolation of the transition points.

This paper is divided in to three sections. In section 2, we discuss our numerical results, and this is divided into eight subsections. Results are discussed and compared with the existing literatures in section 3.

2. Numerical results

In this section, various criteria for the MI transition are discussed. We start with a three dimensional phase diagram in B , Δ and μ parameter space for given $J^z = 0$ and 0.5. Thereafter, various criteria of the MI such as lowest excitation energy Γ , edge spin correlation with its nearest neighbor $C(r = 1)$, local susceptibility at the site nearest neighbor to the edge χ_2 , superconducting or spin-nematic order parameter of edge spin $P(r = 1)$, and structure factor $S(k)$ are studied. We show that all these quantities show extrema at a transition parameter B_m in $\Delta - B$ parameter space. However, all these extrema B_m are extrapolated to the same point in the thermodynamic limit, and this extrapolation is done in the section 2.8. The ES is analyzed in section 2.7 to show the distinction between topological and the Ising phase.

2.1. Phase diagram

A phase diagram of the model Hamiltonian in (5), is shown as a color gradient plot in figure 1, where the color gradient represents the critical value of B_c , and X- and Y-axis are the μ and the Δ of the MI transition points for a system size $N = 100$ for $J^z = 0$. The phase transition in the $\mu - \Delta$ parameter space shows that a finite Δ_c is required to generate the Majorana modes in a finite system. The μ favors the longitudinal degrees of freedom and tries to induce the ferromagnetic order, although B tries to align the nearest spins in opposite directions to induce the

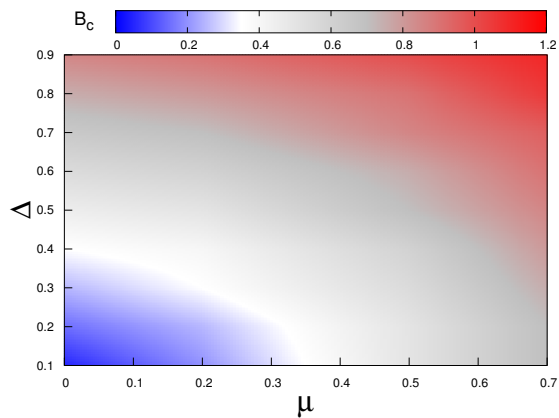


Figure 1. MI phase boundary for a helical liquid mentioned in (5) in the parameter space of Δ and μ for $J^z = 0$. The color gradient represents the critical magnetic field B_c in the phase boundary.

Antiferromagnetic Néel phase. In fact the B and the μ both favor the Ising order, whereas the Δ breaks the parity symmetry and induces the degeneracy in the system. It also induces the formation of Cooper-pairs or magnon-pairs like excitations at the two neighboring sites for the model Hamiltonian given by (6) or (5) respectively. As shown in figure 1, the transition value B_c increases with increasing μ_c for a fixed value of Δ_c , and it increases with increasing Δ_c for a given μ_c , and the trends are similar for both $J^z = 0$ and 0.5. We notice that the Majorana state occurs for $(B - \mu)^2 < \Delta^2$.

2.2. Excitation gap Γ

To characterize the Majorana modes in one dimension for the helical system, the lowest excitation gap Γ is defined as

$$\Gamma = E_1(\Delta, \mu, B) - E_0(\Delta, \mu, B), \quad (9)$$

where E_0 and E_1 are ground state and lowest excited state of the Hamiltonian in (5). The $\Gamma - N$ is plotted in log-linear scale in figure 2. The $\Gamma - N$ plot for $\mu = 0$, $\Delta = 0.5$, $J^z = 0.0$, and for five values of B . For $B = 0.35, 0.4$ and 0.45 , Γ shows the exponential decay (Majorana regime), whereas Γ goes linearly with $1/N$ for $B = 0.5$ and 0.55 (Ising phase) as shown in the figure 2. The phase boundary of MI transition is evaluated based on change in $\Gamma - N$ relation from exponential to the power law. We also notice that the contribution to the excitation gap Γ is uniformly distributed in the Ising phase, whereas, in the Majorana state, the major contribution comes from the edge as shown in Fig. 5 of [35].

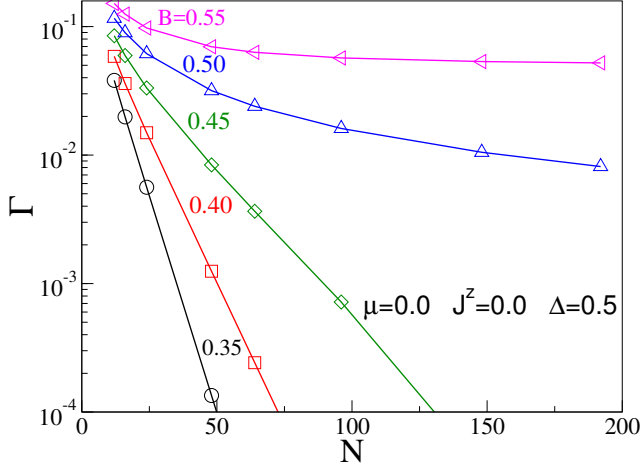


Figure 2. Lowest excitation gap Γ (in (9)) vs. the system size N for $\mu = J^z = 0$ and $\Delta = 0.5$ with different values of B chosen around the $B_c = 0.48$ (see figure 1).

2.3. Correlation function $C(r = 1)$ from the edge

The longitudinal spin-spin correlation fluctuation $C(r)$ at a distance r from reference point i is defined as

$$C(r) = \langle S_i^z S_{i+r}^z \rangle - \langle S_i^z \rangle \langle S_{i+r}^z \rangle, \quad (10)$$

where $\langle S_i^z \rangle$ and $\langle S_{i+r}^z \rangle$ are spin densities at the reference site i and other site $i + r$. In figure 3, the edge spin site $i = 1$ is considered as the reference spin. The distance dependence of $C(r)$ for $\mu = 0$, $J^z = 0$ and $\Delta = 0.5$ is shown in inset of figure 3. It decreases exponentially for $r \geq 2$, and effectively, only last two sites are correlated. Therefore, $C(r = 1)$ between nearest neighbors is important. $C(r = 1)$ first increases with B in the Majorana state and decreases afterwards in the Ising phase. The $dC(r = 1)/dB$ is plotted as a function of B/B_c in the main figure 3 for $(J^z = 0, \Delta = 0.5)$, and $(J^z = 0.5, \Delta = 1.5)$ and $\mu = 0$. This minimum for the given value of parameters is also consistent with the MI transition point calculated from energy degeneracy.

2.4. Local magnetic susceptibility χ_i

The Majorana modes are confined to the edge of the system, therefore we focus on the spin density of edge sites $i = 1$ and 2 for $\Delta = 0.5$, $\mu = 0$ and $J^z = 0$. The spin density and the local staggered magnetic susceptibility is defined as

$$\rho_i = 2 \langle S_i^z \rangle, \quad (11)$$

$$\chi_i = \left| \frac{d\rho_i}{dB} \right|, \quad (12)$$

where, $\langle S_i^z \rangle$ are the longitudinal spin density at site i . The magnitude of spin density ρ_i for site $i = 1, 2$ increases at both the sites with B , it is positive at

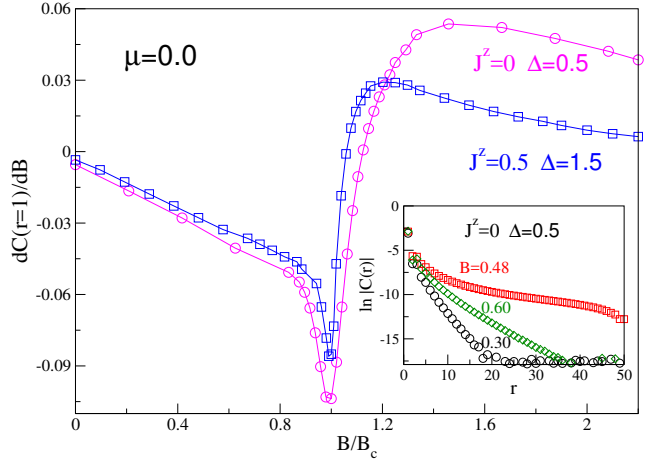


Figure 3. The derivative of longitudinal spin-spin correlation between the spins corresponding to the edge bond $dC(r = 1)/dB$ with the staggered magnetic field B both for $(\Delta = 0.5, \mu = J^z = 0)$ and $(\Delta = 1.5, J^z = 0.5, \mu = 0)$. The inset shows the distance dependence of $\ln |C(r)|$ for $B = 0.3, 0.48$ and 0.6 and for $\Delta = 0.5$, $\mu = J^z = 0$.

site 1 and negative at site 2. The magnitude of ρ_i at site 2 is lower than that is at site 1. However, both of them saturate with high staggered field, but ρ_1 continuously increases and there is no maxima for this function. The χ_2 as a function of B/B_c are plotted in the main figure 4 for $(J^z = 0, \Delta = 0.5)$ and $(J^z = 0.5, \Delta = 1.5)$ and both for $\mu = 0$. These two functions show a maxima near the transition. The ρ_i for the whole system for $J^z = 0, \Delta = 0.5$ and $\mu = 0$ is shown in the inset of figure 4. We notice that the variation of ρ_i is confined to the edge and the first few neighboring sites, and has constant value throughout the rest of system. The ρ_i for $J^z = 0.5, \Delta = 1.5$ and $\mu = 0$ behaves in a similar manner.

2.5. Quadrupolar order parameter $P(r = 1)$

The third term of the Hamiltonian in (5) induces the spin quadrupolar/spin-nematic order in the system. In this phase $\langle S^+ \rangle$ vanishes, whereas $\langle S^+ S^+ \rangle$ has non-zero value, and two magnon pair formation is favored similar to superconductor system where two electrons form Cooper pair. The spin distance dependent quadrupolar order parameter is defined as

$$P(r) = \langle S_i^x S_{i+r}^x \rangle - \langle S_i^y S_{i+r}^y \rangle, \quad (13)$$

$$= \langle S_i^+ S_{i+r}^+ + S_i^- S_{i+r}^- \rangle.$$

$P(r)$ is the difference in the X and Y component of correlation $\langle \vec{S}_i \cdot \vec{S}_{i+r} \rangle$. For $r = 1$, this quantity is very similar to the spin quadrupolar or superconducting order parameter of the spinless fermion model. The $P(r = 1)$ is calculated as a function of B for $(\Delta = 0.5, J^z = 0)$ and $(\Delta = 1.5, J^z = 0.5)$ and both for $\mu = 0$,

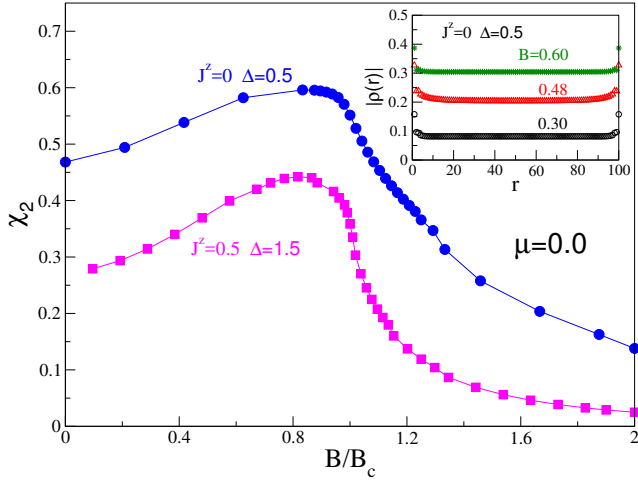


Figure 4. Local staggered magnetic susceptibility (in (12)) of the second site nearest neighbor to the edge χ_2 vs. B/B_c both for $(\Delta = 0.5, \mu = J^z = 0)$ and $(\Delta = 1.5, J^z = 0.5, \mu = 0)$. In the inset, the spin density $\rho(r)$ for the whole system for $B = 0.3, 0.48$ and 0.6 with $\Delta = 0.5, \mu = J^z = 0$ is shown.

and we notice that when Δ dominates over B , the system goes from non-degenerate Ising phase to doubly degenerate states which favors Majorana edge state and the bulk phase goes to spin quadrupolar phase as $P(r) \neq 0$. The $P(r=1)$ first increases with B , and then it saturates with higher B . The derivative of $P(r=1)$ with B for $(\Delta = 0.5, J^z = 0, \mu = 0)$ and $(\Delta = 1.5, J^z = 0.5, \mu = 0)$ shows maxima at $B = 0.48$ and $B = 1.04$ respectively as shown in the main figure 5. The distance dependence of $P(r)$ as a function r are shown for both the regime of the Majorana modes and the Ising states in inset of figure 5. The reference site i is the edge site of the chain. In the Majorana state $P(r)$ shows long range behavior, however, it decays exponentially in case of Ising phase.

2.6. Longitudinal structure factor $S(k)$

The longitudinal structure factor $S(k)$ is the Fourier transformation of $C(r)$ given in (10), and can be defined as

$$S(k) = \sum_r (\langle S_i^z S_{i+r}^z \rangle - \langle S_i^z \rangle \langle S_{i+r}^z \rangle) e^{ikr}. \quad (14)$$

Now let us define a quantity K_ρ in small k limit defined as

$$K_\rho = \frac{S(k)}{k/\pi}; k \rightarrow 0, \quad (15)$$

where $k = \frac{2\pi m}{N}$; $m = 0, \pm 1, \pm 2, \dots, \pm \frac{N}{2}$. K_ρ is proportional to the Luttinger Liquid parameter [53–56]. We take the value of the function $\frac{\pi S(k)}{k}$ at $k = \frac{2\pi}{N}$ ($m = 1$). We calculate K_ρ for the $(\Delta = 0.5,$

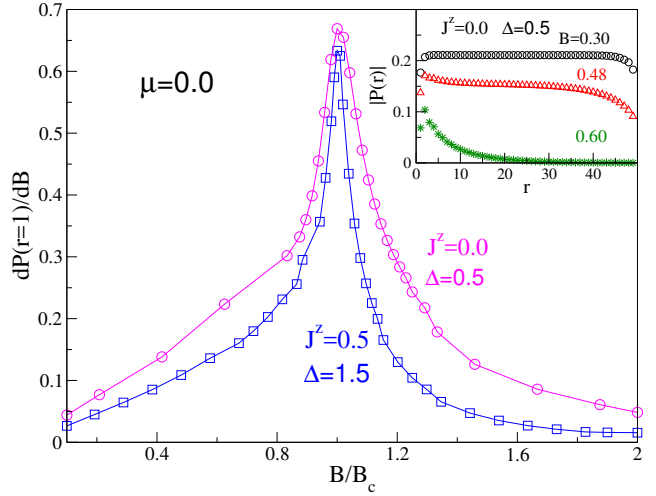


Figure 5. $\frac{dP(r=1)}{dB}$ as a function of $\frac{B}{B_c}$ is shown in the main figure for $(\Delta = 0.5, \mu = J^z = 0)$ and $(\Delta = 1.5, J^z = 0.5, \mu = 0)$. $P(r)$ (in (13)) is plotted for the whole system in the inset for $B = 0.3, 0.48$ and 0.6 with $\Delta = 0.5, \mu = J^z = 0$.

$J^z = 0)$ and $(\Delta = 1.5, J^z = 0.5)$ as a function of μ and B . The derivative of K_ρ as a function of B shows maxima at $B = 0.48, 0.52,$ and 0.7 for $\mu = 0, 0.2$ and 0.5 at $J^z = 0$ and $\Delta = 0.5$. The derivative of K_ρ with B/B_c for $(\Delta = 0.5, J^z = 0)$ and $(\Delta = 1.5, J^z = 0.5)$ is shown for three different values of μ in the main and in the inset of figure 6. The maxima of $\frac{dK_\rho}{dB}$ indicates the boundary between the Majorana and the Ising state. The extrapolated value of the transition point is very close to the transition point calculated from other criteria. It also shows that the critical value of B for the transition calculated from $\frac{dK_\rho}{dB}$ at a fixed Δ increases with increasing μ .

2.7. Entanglement spectrum in Ising and Majorana state

As the Majorana mode is topological in nature, there is no well-defined order parameter. Therefore, direct measurement of this property is not possible [57–59]. Therefore, we study the ES of the reduced density matrix of the system to indirectly study the topological aspect. In this phase, all the states are either doubly or multiply degenerate [57, 58]. The reduced density matrix of a system (half of the full system) can be constructed in the GS of the full system by integrating out the environment degrees of freedom. The eigenvalues of the reduced density matrix are represented as λ_i . The Schmidt gap is defined as $\Delta_S = \lambda_0 - \lambda_1$, where λ_0 and λ_1 are the largest and second largest eigenvalues of the reduced density matrix. Topological phases are also characterized by $\Delta_S = 0$, whereas it is finite in the trivial phase [58]. In a non-topological state the largest eigenvalue is

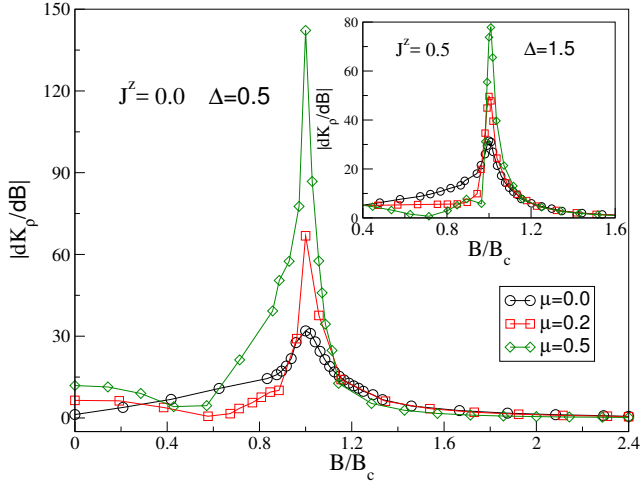


Figure 6. Derivative of K_ρ (in (15)) with the staggered magnetic field B , as a function of $\frac{B}{B_c}$ is shown in the main figure for $\Delta = 0.5$, $J^z = 0$, and the inset shows the same for $\Delta = 1.5$, $J^z = 0.5$ for $\mu = 0, 0.2$ and 0.5 .

non-degenerate and has mixed degenerate and non-degenerate eigenvalues [57, 58].

The ES of the reduced density matrix is analyzed for a chain of $N = 96$ spins with PBC in the deep Ising state, and in the deep Majorana state for $J^z = 0$ and 0.5 . We plot the Schmidt gap as a function of $\frac{\Delta}{\Delta_c}$ for $J^z = 0$ and $J^z = 0.5$ shown in the inset of figure 7 for $\mu = 0$ and $B = 0.5$. We notice that $\lambda_{n=0}$ is non-degenerate in the Ising state and Schmidt gap is finite in this regime but goes to zero in the Majorana state as shown in the inset of figure 7. In the Ising phase many of λ_n are non-degenerate for ($J^z = 0$, $\mu = 0$, $B = 0.5$, $\Delta = 0.2$) and ($J^z = 0.5$, $\mu = 0.0$, $B = 0.5$, $\Delta = 0.7$). In this phase the ES is of mixed type. The spectrum is shown as open and filled symbols in the main figure 7 for $J^z = 0$ and 0.5 respectively. In the Majorana phase the $\lambda_{n=0}$ is triply degenerate, and for other higher n , these are either doubly or multiply degenerate as shown in the main figure 7 for ($J^z = 0$, $\mu = 0$, $B = 0.5$, $\Delta = 0.9$) and ($J^z = 0.5$, $\mu = 0$, $B = 0.5$, $\Delta = 1.2$). The phase boundary of the system can be characterized at the point where Schmidt gap goes to zero and the whole spectrum becomes doubly or multiply degenerate. In the Majorana phase first few largest λ_n are independent of parameters.

2.8. MI phase boundary

In the last seven subsections, different criteria give us different MI phase boundary in a finite system size and the phase boundary B_c , calculated from different criteria have different finite size dependence. For $\mu = 0.2$, the finite size scaling of the B_c for four different criteria, i.e., ground state degeneracy, K_ρ , $P(r = 1)$

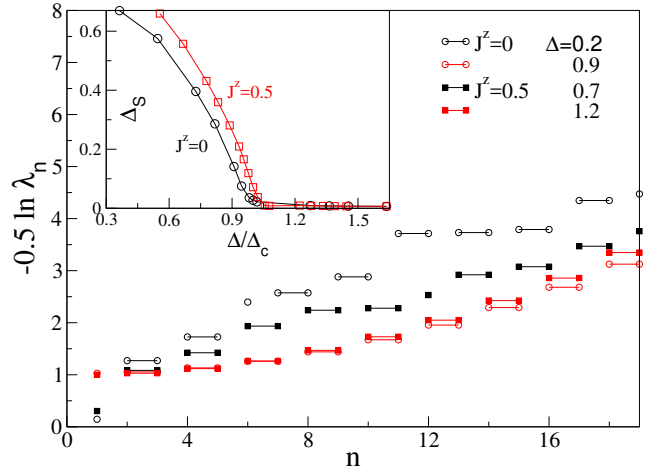


Figure 7. The entanglement spectrum λ_n is plotted for $\mu = 0$ and $B = 0.5$ in both the Ising and Majorana regime for $J^z = 0$ and $J^z = 0.5$ in the main figure. In the inset, the Schmidt gap Δ_S is shown as a function of $\frac{\Delta}{\Delta_c}$ for $B = 0.5$, $\mu = 0$ both for $J^z = 0$ and $J^z = 0.5$.

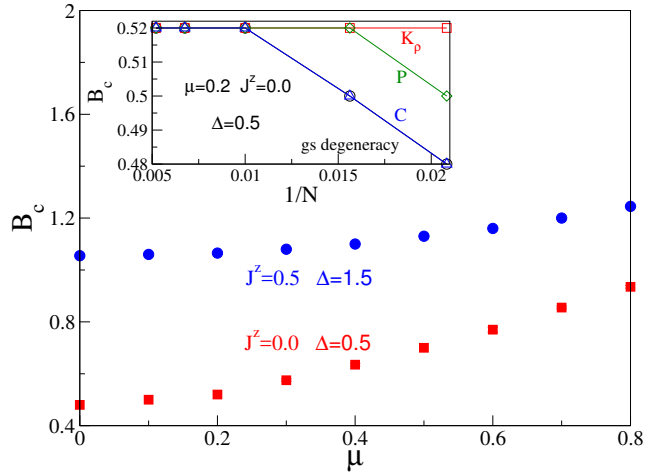


Figure 8. The effect of μ on MI transition in the thermodynamic limit both for $J^z = 0$, $\Delta = 0.5$ and $J^z = 0.5$, $\Delta = 1.5$ are shown in the main figure. The finite size scaling of B_c from different criteria for $J^z = 0$, $\Delta = 0.5$ and $\mu = 0.2$ is shown in the inset.

and $C(r = 1)$ are shown in the inset of figure 8. The ground state degeneracy and $C(r = 1)$ have same finite size effect. We notice that the extrapolation from all the criteria leads to same $B_c = 0.52$ in the thermodynamic limit. The effect of μ on the MI transition point B_c is shown in the thermodynamic limit for ($J^z = 0$, $\Delta = 0.5$) and ($J^z = 0.5$, $\Delta = 1.5$) in the main figure 8.

3. Discussion

We have studied the helical liquid system and mapped this model into a XYZ spin-1/2 chain model. The Majorana-Ising transition is characterized by calculating the lowest excitation gap of the model Hamiltonian in (5) on a chain geometry. In the Majorana state, the system has finite gap for a finite system which decays exponentially with the system size N . The closing of the gap in the thermodynamic limit is consistent with the study by Sela et al. [31]. Our aim of this paper is to explore various criteria to characterize Majorana mode other than closing of the lowest excitation gap, and the accurate determination of the MI transition boundary. We have calculated various quantities, e.g., ρ_i , $C(r)$, $P(r)$, K_ρ , Δ_S . We have shown that the phase boundary calculated from the various criteria are the same for given value of Δ and μ in the thermodynamic limit. We have shown that in strong repulsive interaction limit $J^z > 0$, Majorana mode occurs at higher value of Δ than the non-interacting case ($J^z = 0$), which is consistent with the study of Gangadharaiyah et al. [30], where they have shown that the repulsive interaction weakens the Majorana modes. The J^z term of (5) is similar to the repulsive interaction term of the spinless fermion model in (6). In the mean field limit, J^z term reduces to effective μ . We have noticed that the Majorana state occurs for $(\mu - B)^2 < \Delta^2$, therefore, any change in μ changes the value of critical field B_c . The $P(r)$ is long range in the Majorana state, whereas it decays exponentially in the Ising phase as shown in the inset of figure 5. In the Majorana state, the bulk of system shows quadrupolar/or spin nematic phase like behavior. The local magnetic susceptibility χ of the edge sites shows maxima near the phase boundary.

We have also studied the ES of this model, and it is shown that the Ising phase has finite Schmidt gap Δ_S , and non-degenerate eigenvalues are present in the spectrum of the reduced density matrix of the system, whereas the topological aspect of Majorana state is characterized by the doubly degenerate eigenvalues and zero Schmidt gap [57, 58]. We have also shown that ES of the reduced density matrix of the ground state shows double and multiple degeneracy in the Majorana state. We have also noticed threefold degeneracy in the largest eigenvalues in this state in the thermodynamic limit. Degeneracy of all the eigenvalues is very similar to the study by Pollmann et al. [57] to distinguish the topological and trivial phase of $S = 1$ system. The first few eigenvalues of ES in the Majorana state is almost independent of parameters as shown in figure 7.

In conclusion, we have studied the helical liquid phase in one dimensional system. This system shows the Majorana-Ising transition, and the phase boundary is calculated using various criteria. The topological

aspect of the Majorana modes is studied for helical model, and the closing of the Schmidt gap and degeneracy of full spectrum of reduced density matrix can also be used to characterize the phase boundary of Majorana-Ising transition. This model is one of the most interesting and a general model for spin-1/2 systems. Our study shows that an anisotropic spin-1/2 chain can be a good candidate to observe the Majorana modes and MI transition. The local experimental probe like neutron magnetic resonance can be used to measure the local spin density at the edge of the sample.

Acknowledgments

MK thanks Z. G. Soos and Sumanta Tewari for their valuable comments. MK thanks DST for a Ramanujan Fellowship SR/S2/RJN-69/2012 and funding computation facility through SNB/MK/14-15/137. SS thanks the DST (SERB, SR/S2/LOP-07/2012) fund and SNBNCBC for supporting the visit.

References

- [1] Majorana E 1937 *Nuovo Cimento* **14** 171
- [2] Wilczek F 2009 *Nat. Phys.* **5** 614
- [3] Bernevig B A and Hughes T L 2013 *Topological Insulators and Topological Superconductors* (Princeton: Princeton University Press)
- [4] Ivanov D A 2001 *Phys. Rev. Lett.* **86** 268–271
- [5] Kraus Y E, Auerbach A, Fertig H A and Simon S H 2009 *Phys. Rev. B* **79** 134515
- [6] Wimmer M, Akhmerov A R, Medvedyeva M V, Tworzydło J and Beenakker C W J 2010 *Phys. Rev. Lett.* **105** 046803
- [7] Sato M and Fujimoto S 2016 *J. Phys. Soc. Jpn.* **85** 072001
- [8] Stanescu T D and Tewari S 2013 *Journal of Physics: Condensed Matter* **25** 233201
- [9] Mourik V, Zuo K, Frolov S M, Plissard S R, Bakkers E P A M and Kouwenhoven L P 2012 *Science* **336** 1003–1007
- [10] Deng M T, Yu C L, Huang G Y, Larsson M, Caroff P and Xu H Q 2012 *Nano Lett.* **12** 6414–6419
- [11] Rokhinson L P, Liu X and Furdyna J K 2012 *Nat. Phys.* **8** 795
- [12] Das A, Ronen Y, Most Y, Oreg Y, Heiblum M and Shtrikman H 2012 *Nat. Phys.* **8** 887
- [13] Finck A D K, Van Harlingen D J, Mohseni P K, Jung K and Li X 2013 *Phys. Rev. Lett.* **110** 126406
- [14] Jafari R, Langari A, Akbari A and Kim K S 2017 *J. Phys. Soc. Jpn.* **86** 024008
- [15] Kitaev A Y 2001 *Physics-Uspekhi* **44** 131
- [16] Fu L and Kane C L 2008 *Phys. Rev. Lett.* **100** 096407
- [17] Fu L and Kane C L 2009 *Phys. Rev. B* **79** 161408
- [18] Alicea J 2010 *Phys. Rev. B* **81** 125318
- [19] Alicea J *Rep. Prog. Phys.* **75** 076501
- [20] Sau J D, Lutchyn R M, Tewari S and Das Sarma S 2010 *Phys. Rev. Lett.* **104**(4) 040502 URL <https://link.aps.org/doi/10.1103/PhysRevLett.104.040502>
- [21] Potter A C and Lee P A 2010 *Phys. Rev. Lett.* **105** 227003
- [22] Stoudenmire E M, Alicea J, Starykh O A and Fisher M P 2011 *Phys. Rev. B* **84** 014503
- [23] Fukui T and Fujiwara T 2010 *J. Phys. Soc. Jpn.* **79** 033701
- [24] Sarkar S 2017 *Sci. Rep.* **7** 1840

- [25] Zhang C, Tewari S, Lutchyn R M and Das Sarma S 2008 *Phys. Rev. Lett.* **101** 160401
- [26] Jiang L, Kitagawa T, Alicea J, Akhmerov A R, Pekker D, Refael G, Cirac J I, Demler E, Lukin M D and Zoller P 2011 *Phys. Rev. Lett.* **106** 220402
- [27] Nayak C, Simon S H, Stern A, Freedman M and Das Sarma S 2008 *Rev. Mod. Phys.* **80** 1083–1159
- [28] Sau J D, Tewari S and Das Sarma S 2010 *Phys. Rev. A* **82**(5) 052322
- [29] Alicea J, Oreg Y, Refael G, von Oppen F and Fisher M P A 2011 *Nat. Phys.* **7** 412
- [30] Gangadharaiah S, Braunecker B, Simon P and Loss D 2011 *Phys. Rev. Lett.* **107** 036801
- [31] Sela E, Altland A and Rosch A 2011 *Phys. Rev. B* **84** 085114
- [32] Sarkar S 2016 *Sci. Rep.* **6** 30569
- [33] Qi X L and Zhang S C 2010 *Phys. Today* **63** 33
- [34] Qi X L and Zhang S C 2011 *Rev. Mod. Phys.* **83** 1057–1110
- [35] Dey D, Saha S K, Deo P S, Kumar M and Sarkar S 2017 *J. Phys. Soc. Jpn.* **86** 074002
- [36] Wu C, Bernevig B A and Zhang S C 2006 *Phys. Rev. Lett.* **96** 106401
- [37] Fradkin E 2013 *Field Theories of Condensed Matter Physics* (Cambridge University Press)
- [38] Katsura H, Schuricht D and Takahashi M 2015 *Phys. Rev. B* **92**(11) 115137
- [39] Kawabata K, Kobayashi R, Wu N and Katsura H 2017 *Phys. Rev. B* **95**(19) 195140
- [40] Gergs N M, Fritz L and Schuricht D 2016 *Phys. Rev. B* **93** 075129
- [41] Rahmani A, Zhu X, Franz M and Affleck I 2015 *Phys. Rev. B* **92** 235123
- [42] Zhu W, Gong S S, Haldane F D M and Sheng D N 2015 *Phys. Rev. B* **92** 165106
- [43] Ejima S and Fehske H 2015 *Phys. Rev. B* **91** 045121
- [44] Parvej A and Kumar M 2017 *Phys. Rev. B* **96**(5) 054413
- [45] Luo C, Datta T and Yao D X 2016 *Phys. Rev. B* **93**(23) 235148
- [46] Gong S S, Zhu W, Sheng D N and Yang K 2017 *Phys. Rev. B* **95**(20) 205132
- [47] White S R 1992 *Phys. Rev. Lett.* **69** 2863–2866 URL <http://link.aps.org/doi/10.1103/PhysRevLett.69.2863>
- [48] White S R 1993 *Phys. Rev. B* **48** 10345–10356
- [49] Dey D, Maiti D and Kumar M 2016 *Papers in Physics* **8**
- [50] Kumar M, Soos Z G, Sen D and Ramasesha S 2010 *Phys. Rev. B* **81**(10) 104406
- [51] Kumar M, Parvej A, Thomas S, Ramasesha S and Soos Z G 2016 *Phys. Rev. B* **93** 075107
- [52] Kumar M, Ramasesha S and Soos Z G 2012 *Phys. Rev. B* **85** 134415
- [53] Clay R T, Sandvik A W and Campbell D K 1999 *Phys. Rev. B* **59**(7) 4665–4679
- [54] Ejima S, Gebhard F and Nishimoto S 2005 *EPL (Europhysics Letters)* **70** 492 URL <http://stacks.iop.org/0295-5075/70/i=4/a=492>
- [55] Cheng C, Mao B B, Chen F Z and Luo H G 2015 *EPL (Europhysics Letters)* **110** 37002
- [56] Hu H, Cheng C, Wang Y, Luo H G and Chen S 2015
- [57] Pollmann F, Turner A M, Berg E and Oshikawa M 2010 *Phys. Rev. B* **81** 064439
- [58] Guang-Hua L, Yu Z and Guang-Shan T 2014 *Communications in Theoretical Physics* **61** 759
- [59] Chandran A, Khemani V and Sondhi S L 2014 *Phys. Rev. Lett.* **113** 060501